Practical Entropy Loading Enabled by Enumerative Sphere Shaping with Short Block Lengths

Yizhao Chen[1], Weihao Li[2], Junda Chen[2], Yating Xiang[2], Mingming Zhang[2], Deming Liu[1,2] and Ming Tang[2*]
[1] School of Cyber Science and Engineering, Huazhong University of Science and Technology, Wuhan, 430074, China,
[2] Wuhan National Lab for Optoelectronics (WNLO) & National Engineering Laboratory for Next Generation Internet Access System, School of Optical and Electronic Information, Huazhong University of Science and Technology, Wuhan, 430074, China
**tangming@mail.hust.edu.cn*

Abstract: We propose a practical entropy loading scheme using enumerative sphere shaping, providing considerable shaping gain even with ultra-short block lengths. In the experimental validation, up to 6.0% capacity improvement is achieved.

1. Introduction

Along with the development of high-end technologies (e.g. high-definition video, cloud computing, social networking, etc.), the past decade has witnessed exponential growth of data demand for fiber optic communication. Probabilistic shaping (PS), benefiting from its shaping gain and flexible information rates, has attracted extensive interest among both academics and service suppliers in recent years [1,2]. In particular, PS enabled entropy loading (EL) was proposed to load continuous entropies instead of discrete bit levels to subcarriers in multicarrier systems [3], providing tunable information rates for the flexible network implementation. The efficiency of EL has been proven the optimum capacity-approaching solution for bandwidth-limited channels [4]. However, the practical shaping algorithms for EL with acceptable complexity are rarely discussed. Constant composition distribution matcher (CCDM) is the most popular shaping algorithm, and has been employed in the experimental demonstration of EL [5,6]. As CCDM required large block lengths to work well, its practical application in multicarrier transmission faces the challenge of throughput and computational complexity. Recent years, many other shaping methods suitable for short-block-length applications have been proposed, such as hierarchical distribution matcher (HiDM), multiset-partition distribution matching (MPDM), and enumerative sphere shaping (ESS) [7]. Among them, ESS is capable of minimizing the rate loss at any block length, providing a potential solution for EL.

In this work, we propose a practical EL scheme using ESS with short block lengths, permitting its high-throughput and high-capacity application in multicarrier systems. The ESS is first theoretically compared with the CCDM in terms of the achievable information rate (AIR) and net information rate (NIR). Then, an experimental validation is carried out in a single sideband (SSB) discrete multi-tone (DMT) system, in which the ESS-based EL is compared with the CCDM-based EL and the conventional bit and power loading (BPL) scheme based on Levin-Campello (LC) algorithm. As a result, ESS achieves up to 3.4% and 6.0% capacity improvement for the block lengths of 200 and 100, respectively.

2. Operational Principles

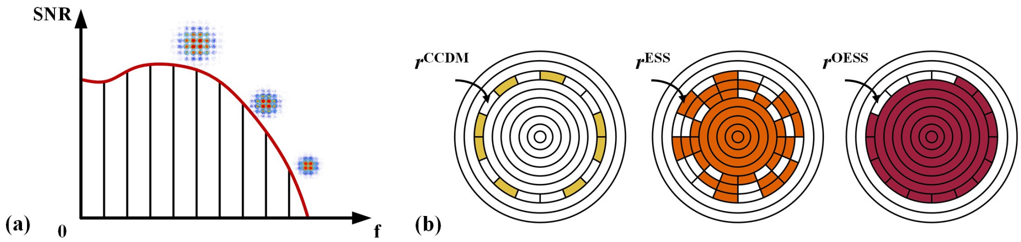

Fig. 1. (a) Entropy loading for multicarrier systems. (b). Geometric representation in 2-dimention of CCDM, ESS and OESS.

For a wide-bandwidth optical transmission system, a flat end-to-end system frequency response is rarely obtained due to the influence of device bandwidth, nonlinear equalization and pulse-shaping. Thus, the overall signal-to-noise ratio (SNR) usually fluctuates along different subcarriers. To take advantage of the spectral resource, the conventional BPL scheme assign different modulation formats to the subcarriers according to their SNRs. With the development of PS, the EL is proposed by loading the PS-QAM with specific entropy to each subcarrier as shown in Fig.1 (a), achieving better capacity performance compared with BPL. To achieve high-throughput implementation in multicarrier systems, the shaping algorithms is highly desired to work well in parallel with small block lengths. However, the shaping algorithms for EL has not been intensively investigated.

The widely employed CCDM outputs sequences with the same compositions to promise an intended probability distribution, for which Maxwell-Boltzmann (MB) distribution is usually utilized. Thus, the CCDM only allows partial sequences located on the surface of an N-dimensional sphere, as shown in Fig.1 (b). Consequently, many sequences with the same or lower energy are abandoned by CCDM, degrading its power efficiency in the finite-block-length regime. In other words, CCDM suffers from high rate losses with small block lengths. By contrast, ESS can achieve superior performance with small block length by utilizing all sequences bounded by an energy constraint $E_{\max}$, as shown in Fig.1 (b). Moreover, optimized ESS (OESS) is proposed to further improve the power efficiency [8]. To perform practical EL implementation, ESS is more suitable than CCDM to serve as the shaping algorithms.

The performance of ESS and CCDM with finite block lengths can be numerically analyzed by counting their rate loss, AIR and NIR. The shaping rates of ESS and CCDM can be denoted by

$$R_{\mathrm{S}} = k/N = \begin{cases} \left\lfloor \log_2 \left(N! \middle/ \prod n_i! \right) \right\rfloor / N, & \text{(CCDM)} \\ \left\lfloor \log_2 |S| \right\rfloor / N, & \text{(ESS/OESS)} \end{cases}, \tag{1}$$

where k and N denote the input block length and the output block length. For CCDM, $n_i = N \cdot P_X(\alpha)$ represents the numbers of the output compositions, where $P_X(\alpha)$ is the probability of the corresponding output element α. For ESS, S represents the set of all sequences in the energy constraint $E_{\max}$. Their rate loss can be calculated by

$$R_{\text{loss}} \triangleq H(X_{\mathrm{MB}}) - R_S, \tag{2}$$

where X_{MB} represents the MB-distributed random variable with the same average energy as the output sequences. The finite block length AIR for 2^m-QAM signals is defined as

$$\mathrm{AIR}_{\mathrm{N}} = \underbrace{\left[H(C) - \sum_{i=1}^{m} H(C_i \mid Y) \right]}_{\mathrm{AIR}} - 2R_{\text{loss}}, \tag{3}$$

where $H(\cdot)$ denotes entropy. To get the NIR, a concatenated code of 20% LDPC code in DVB-S2 standard and 6.25% staircase code is chosen as the FEC code. Error-free decoding can be verified by the normalized generalized mutual information (NGMI). The NIR can be formulated as

$$R_N = mc - m + 2 + 2R_{\mathrm{S}}, \tag{4}$$

where m denotes the modulation format and c denotes the total code rate.

The numerical comparison of CCDM, ESS and OESS for PS-256QAM is shown in Fig. 2, in which the CCDM with $N = 10000$ serves as an ideal counterpart. As OESS only shows its superiority at ultra-short block lengths, it is investigated with $N = 20$. As shown in Fig. 2(a), ESS achieves lower rate losses than CCDM, especially at high shaping rate. The rate loss of ESS can be reduced by up to 0.185 and 0.107 bits/amp compared with CCDM for the block lengths of 100 and 200, respectively. Note that even OESS with $N = 20$ can outperform CCDM with $N = 200$ in the high-shaping-rate regime. Moreover, by optimizing the shaping parameter for each shaping scheme over a large SNR range from 10 dB to 22 dB in an additive white Gaussian noise (AWGN) channel, their AIR curves are depicted in Fig. 2(b). The ESS achieves better AIR performance than ESS for the same block lengths. And OESS with $N = 20$ performs comparable performance with CCDM with $N = 200$. To gain more insight, the NIR curves is shown in Fig. 3(c) by employing the NGMI threshold of 0.858, and will be used for the EL in the following experiments. Similarly, ESS still keeps better performance compared with CCDM for the same block lengths.

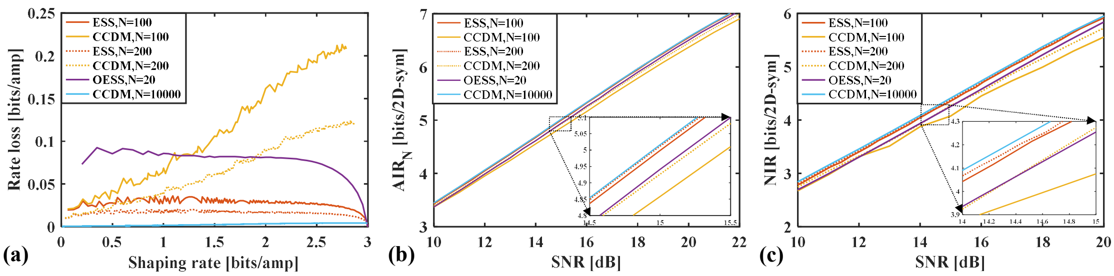

Fig. 2. (a) Comparison of ESS and CCDM in terms of rate loss. (b). AIR versus SNR for an AWGN channel. (c). NIR versus SNR.

3. Experimental Results

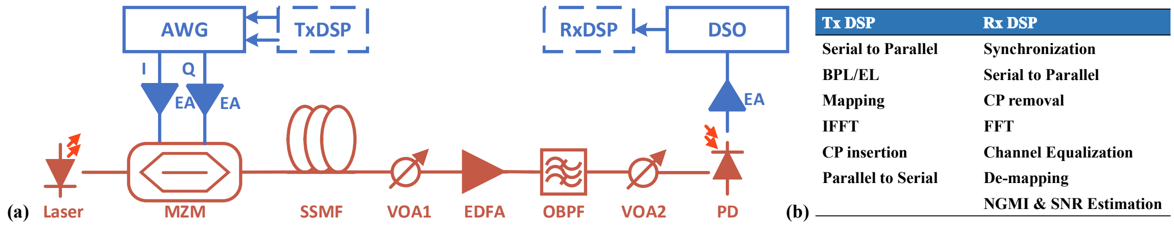

Fig. 3. (a) The experimental setup of SSB DMT systems. (b) The flow diagram of the digital signal processing (DSP).

The experimental setup of SSB DMT systems is shown in Fig. 3 (a). The FFT points and data subcarriers are 512 and 240, respectively. A DMT frame consists of 1 synchronization training symbol (TS), 19 channel estimation TSs and 200 payload symbols. And 20 samples of cyclic prefix (CP) are inserted. DFT matrix is adopted as the precoding matrix. The output digital signal is sampled by an AWG (Keysight M8196, 40 GSa/s). Then, the SSB signal is modulated on the light emitted from a tunable laser source (~100 kHz linewidth) by a DD-MZM (Fujitsu FTM7937EZ611). After 75km standard single mode fiber (SSMF) transmission, a variable optical attenuator (VOA) is deployed in front of the EDFA (Accelink OLP-EDFA-VGA) to manage the received optical power (ROP). The VOA2 is utilized to stabilize the optical power ahead of the photodiode detector (PD) at 1 dBm due to the poor sensitivity of the PD. Finally, the signal is captured by a digital storage oscilloscope (DSO, Lecroy 10-36Zi-A).

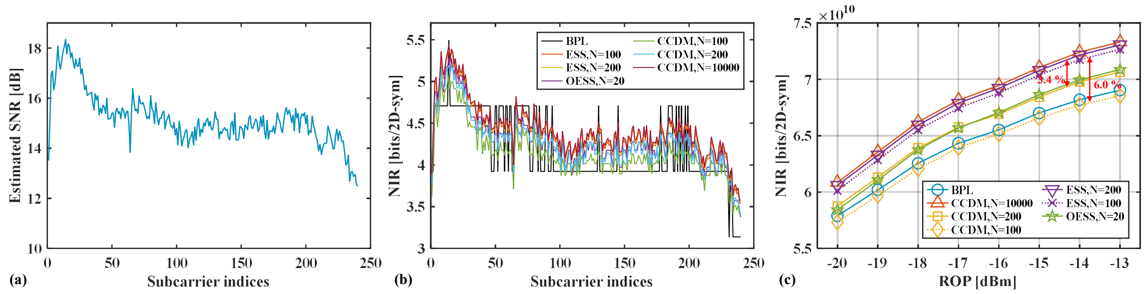

Fig. 4. (a) Estimated SNR. (b) Loaded NIR for each subcarrier by CCDM and ESS (c). The total NIR versus ROP for CCDM and ESS.

First, the estimated SNR for all employed subcarriers with ROP of -13 dBm is shown in Fig. 4(a). Second, subcarriers are loaded with properly shaped 256-QAM signals, according to the pre-estimated SNR and the NIR versus SNR in AWGN channels. And their NIRs are depicted in Fig .4(b). As the conventional BPL can only load discrete modulation formats, the EL based on ESS or CCDM performs continuous NIR loading over all subcarriers. Last, by scanning the ROP, the total NIR versus ROP of BPL and EL based on ESS and CCDM is depicted in Fig. 4(c). As a result, ESS achieves NIR improvements of up to 3.4% and 6.0% compared with CCDM for the block lengths of 200 and 100, respectively. Note that the CCDM with $N = 100$ is even inferior to the conventional BPL scheme. And the OESS with an ultra-short block length of 20 achieves considerable performance and is comparable with the CCDM with $N = 200$.

4. Conclusions

By employing ESS with well performance at short block lengths, a practical solution for EL is proposed for multicarrier systems. The numerical analysis shows that ESS outperforms CCDM with the same block lengths in terms of rate loss, AIR, and NIR. In the experimental validation in a SSB DMT system, ESS-based EL achieves up to 3.4% and 6.0% NIR improvement compared with CCDM-based EL with the block length of 200 and 100, respectively. Moreover, the experimental results show that the CCDM-based EL with a short block length of 100 is even inferior to the conventional BPL scheme. On the contrary, the OESS with an ultra-short block length of 20 can still promise considerable shaping gain.

This work is supported by the National Key R&D Program of China 2018YFB1801205 and NSFC under Grants 61931010.

5. References

[1] F. Buchali, et al., J. Lightwave Technol., 34(7), 2016.
[2] G. Bocherer, et al., IEEE Trans. Commun., 63(12), 2015.
[3] D. Che and W. Shieh, J. Lightwave Technol., 36(1), 2018.
[4] D. Che and W. Shieh, Optics express, 27(7), 2019.
[5] P. Schulte and G. Bocherer, IEEE Trans. Inf. Theory 62(1), 2016.
[6] C. Xie, et al., Opt. Express 26(1), 2018.
[7] Y. C. Gültekin, et al. IEEE Trans. Wireless Commun., 19(2), 2020.
[8] Y. C. Gültekin, et al. IEEE Commun. Letters, 25(4), 2021.